High resolution spectroscopy of Ar–CH_4 and Kr–CH_4 in the 7 μ region ($j = 1 \leftarrow 0$ transition)

I. Pak[a,b], D. A. Roth[a], M. Hepp[a], G. Winnewisser[a], D. Scouteris[c], B. J. Howard[c], and K. M. T. Yamada[d]

[a] I. Physikalisches Institut, Universität zu Köln, Zülpicher Str. 77, 50937, Köln, Germany
[b] Institute of Spectroscopy, Russian Academy of Sciences, 142092, Troitsk, Moscow Region, Russia
[c] Physical and Theoretical Chemistry Laboratory, Oxford University, South Park Road, Oxford QX1 3QZ, United Kingdom
[d] National Institute for Advanced Interdisciplinary Research, Higashi 1-1-4, Tsukuba, Ibaraki 305, Japan

Z. Naturforsch. **53 a,** 725–732 (1998); received May 25, 1998

Diode laser spectra of the rare gas – spherical top van der Waals complexes Ar–CH_4 and Kr–CH_4 were measured in the wavelength region near 1310 cm^{-1} and assigned. The most prominent lines of both complexes exhibit three dense but well resolved $^RP_0$, $^QR_0$, and $^RQ_0$ branches, correlated to the $R(0)$ transition of the triply degenerate bending vibration ν_4 of methane, CH_4. A model Hamiltonian based on Coriolis coupled states was applied for the assignment, analysis and fitting of the spectra to within the experimental accuracy of ≈ 15 MHz. The rotational B constants of the upper and lower states determined from the three allowed branches appeared to be strongly correlated. The precision in the determination of the rotational B constants of the two complexes was substantially increased by additional recording of several weak transitions in the nearly forbidden $^QP_0$ and $^RR_0$ branches, which were fitted together with the allowed transitions. The separation between the rare gas atom and the methane molecule in the ground vibrational state was determined to be 3.999 Å and 4.094 Å for Ar–CH_4 and Kr–CH_4, respectively. The measured small values of the splitting between the K=0 and the $K = \pm 1$ levels in the vibrationally excited state (0.39 cm^{-1} and 0.67 cm^{-1} for Ar–CH_4 and Kr–CH_4, respectively), which characterizes the anisotropy of the intermolecular potential, indicated that Kr–CH_4 and Ar–CH_4 together with Ne–SiH_4 represent examples close to the free rotor limit, where the spherical top CH_4 is almost free to rotate within the complex. In comparison, the previously analyzed Ar–SiH_4 van der Waals molecule is closer to the hindered rotor limit.

1. Introduction

The infrared spectra of Ar–CH_4 and Kr–CH_4 complexes in the 3 μm region, *i. e.* the transitions associated with the ν_3 fundamental band of the triply degenerate stretching vibration of the CH_4 monomer, were recorded first by McKellar, using a Fourier transform spectrometer equipped with a low temperature long path cell [1]. Jet spectra of Ar–CH_4 at even lower temperature in the same spectral range were detected by Lovejoy and Nesbitt [2], Block and Miller [3], and Howard with co–workers [4]. However, being limited by the line broadening due to the fast predissociation, the rotational structure of the spectra was not sufficiently resolved, and therefore the spectra remained unassigned. Instead of looking at the region of the stretching vibration of the CH_4 monomer, we focused on searching the bending vibration region at longer wavelength near 1310 cm^{-1}. As reported in our previous papers [5, 6], the rotationally resolved infrared spectra of the Ar–CH_4 and Kr–CH_4 complexes in the 7 μm region were recorded by diode laser spectroscopy in a supersonic jet.

The structure of the observed spectra was found to be very anomalous compared to other known spectra of similar complexes, although it showed resemblance to that observed by McKellar[1] in the 3 μm band. Both the 3 μm and 7 μm spectra of Ar–CH_4 and Kr–CH_4 were quite different from those of the

Reprint requests to Prof. G. Winnewisser;
E-mail: winnewisser@ph1.uni-koeln.de.

0932-0784 / 98 / 0800-0725 $ 06.00 © – Verlag der Zeitschrift für Naturforschung, D-72072 Tübingen

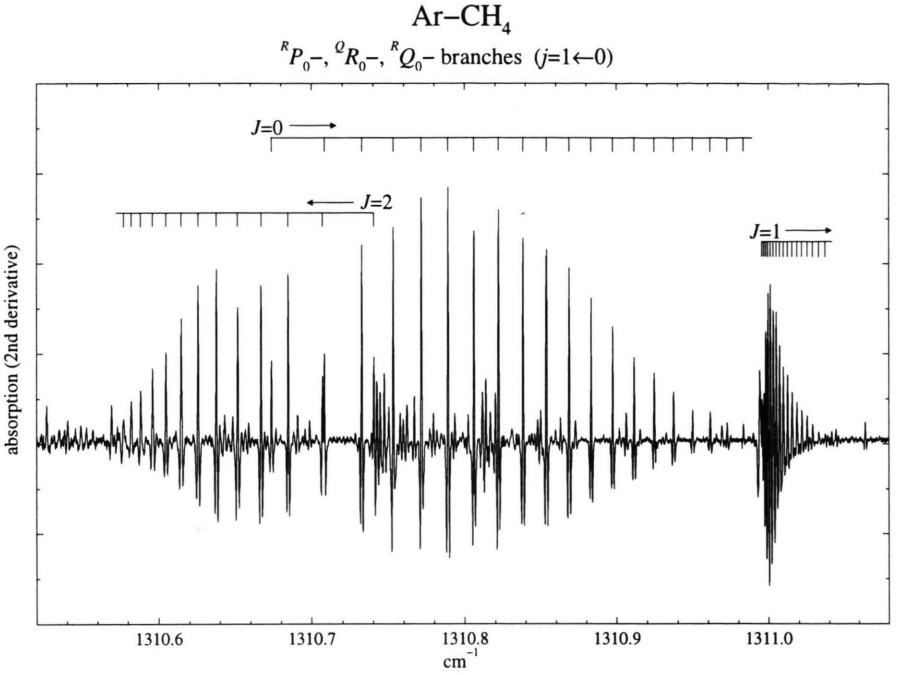

Fig. 1. Allowed Ar–CH_4 transitions correlating to CH_4 R(0). The assignment of the corresponding branches is indicated by their respective first lines (J = 2 for $^{R}P_0$, J = 0 for $^{Q}R_0$, and J = 1 for $^{R}Q_0$).

other known complexes of a rare gas atom and a tetrahedral molecule, such as Ar–CF_4 [7], Kr–CF_4 [7], Ar–NH_4^+ [8, 9], and Ar–SiH_4 [10]. The most similar to the Ar–CH_4 and Kr–CH_4 spectra in the 7 μm region is the Ne–SiH_4 spectrum at 5 μm, which was recently investigated and assigned by Brooks *et al.* [11, 12], using the approach previously developed by Randall *et al.* [13]. The characteristic feature of these spectra was the absence of the familiar rotational structures of rigid symmetric or spherical tops, *i. e.* compact Q branches, framed by regularly spaced P and R branches.

In this paper we present a theoretical consideration of the rovibrational states of these complexes and the assignment of the observed transitions in the range of the R(0) line of methane. The effective Hamiltonian used in this analysis is similar to the one applied in the Ne–SiH_4 case. We emphasize here that the present paper supersedes our tentative assignment given earlier for the Ar–CH_4 case [5].

2. Experimental

The Cologne tunable diode laser (TDL) spectrometer and the experimental procedure were described in details in [6, 14]. Therefore, only a short description is given below.

One of the modes of the TDL was selected by a low resolution grating monochromator. With the aid of beamsplitters, a small part of the laser radiation was tapped for the simultaneous recording of a reference spectrum and for obtaining calibration fringes, produced by a Fabry-Perot etalon with 300 MHz free spectral range. The main part of the TDL beam was directed into a vacuum chamber which contained the supersonic jet. The optical path through the absorbing region in the jet was increased using White type multireflection optics with a base length of 120 mm. The optics were adjusted for 16 passes. The required mixture of methane (typically from 5 to 10% of CH_4) with Ar or Kr was prepared with the aid of two mass flow controllers and injected simultaneously into the vacuum chamber through a pulsed slit nozzle (15 μm width, 20 to 40 mm length) at a repetition rate of 80 Hz. The gas from the chamber was evacuated by a 250 m^3/h roots pump backed by a double stage rotary pump. At a typical stagnation pressure of 2 atm the background pressure in the chamber was kept at a level of 0.1 mbar.

After passing the jet, the TDL radiation was registered by a HgCdTe detector. The wavelength of the TDL was modulated with a 10 kHz sinewave. The signal after preamplification was demodulated by a lock–in amplifier, synchronized with the 10 kHz

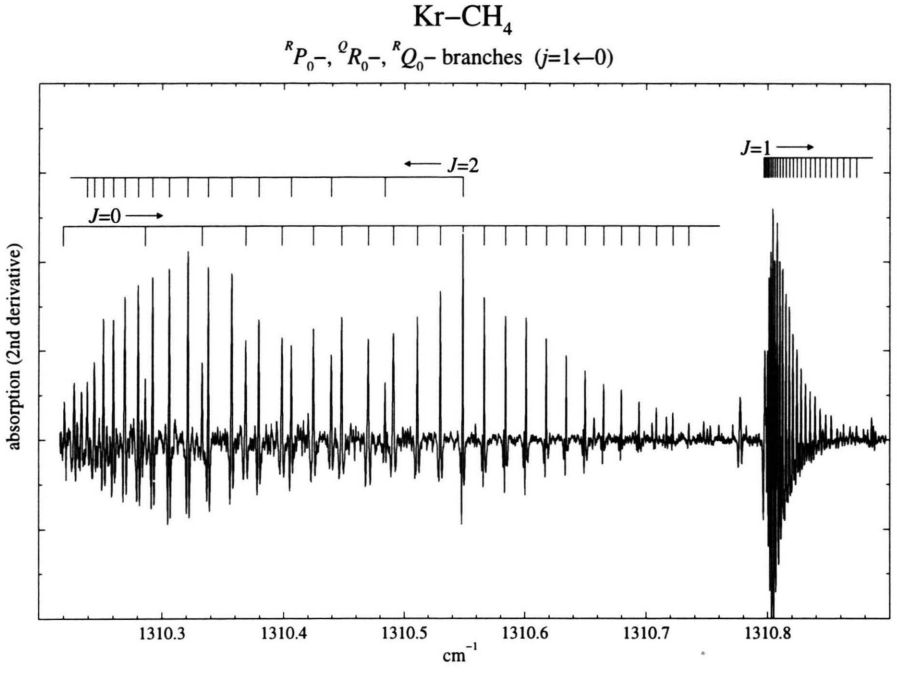

Fig. 2. Allowed Kr–CH_4 transitions correlating to CH_4 R(0). The first lines in the corresponding branches (J = 2 for $^{R}P_0$, J = 0 for $^{Q}R_0$, and J = 1 for $^{R}Q_0$) are indicated.

modulation frequency. The lock–in amplifier operated in the $2f$– mode with a time constant of 0.7 ms. The output of the lock-in was then processed by the boxcar integrator. The timing of the two gates of the boxcar integrator were set shortly before the jet pulse and during the pulse, followed by an appropriate subtraction of the two registered signals performed within the boxcar. This double modulation technique enabled effective reduction of both the low frequency excess noise and the interference base line distortions of the TDL.

3. Results

For both Ar–CH_4 and Kr–CH_4, the bands observed are in the same region as the R(0) transition of the monomer (1311.430 cm^{-1}) and they correlate with the same transition of the monomer (j = 1 ← 0) within the two complexes. The corresponding bands are shown in Figs. 1 and 2. As it was already stated in our paper on the detection of these TDL spectra [5], they resemble closely those, one would expect for perpendicular spectrum originating between a $^1\Sigma$ and a $^3\Sigma$ state of a diatomic molecule in the Hund's case b limit. However, there occurred small but subtle discrepancies in the fit for Ar–CH_4, with increasing tendency for Kr–CH_4. Now the spectra are best analyzed in terms of the theory developed by Brooks *et al.* for Ne–SiH_4 [11]. In this model we consider the coupling of the hindered rotation of the monomer to the rotation of the complex. The Hamiltonian for the system is given by

$$\mathcal{H} = \frac{\hbar^2}{2\mu}\left(-\frac{\partial^2}{\partial R^2} + \frac{(\boldsymbol{J}-\boldsymbol{j})^2}{R^2}\right) + \mathcal{H}_{\text{mon}} + V(R,\theta,\chi), \quad (1)$$

where the terms represent respectively the stretching of the intermolecular bond designated by R, the rotation of the complex and the Hamiltonian of the monomer, while $\boldsymbol{J}$ and $\boldsymbol{j}$ are used for designation of the total angular momentum of the complex and of the angular momentum of the methane part. The last term represents the intermolecular potential $V(R,\theta,\chi)$, which hinders the free rotation of the monomer. The potential V is a function of the intermolecular separation, R, and the orientation of the tetrahedral molecule with respect to the intermolecular axis, described by the two angles θ and χ. In the limit of fairly low anisotropy of the potential V, j is still a fairly good label of the angular momentum of each monomer state of methane and this is coupled to the intermolecular axis with component K. Thus, the j = 0 states are just shifted in energy by the potential, but the j = 1 rotational states are also split into K = 0

and $K = \pm 1$ levels. As shown in [10], the expansion of the rotational function, $(\boldsymbol{J} - \boldsymbol{j})^2$, gives rise to Coriolis terms, which mix states of different K and in the limit of small K–splitting can dramatically alter the energy levels. This causes decoupling of the angular momentum $\boldsymbol{j}$ from the intermolecular axis, and it might be thought that a different angular momentum scheme would be more appropriate. However, as discussed by Brookes *et al.* [11, 12], tetrahedral complexes are unusual. There are no first order effects of the anisotropy of the intermolecular potential in states arising from $j = 1$. As a result, all splittings occur as a consequence of mixing of states with different values of j. Hence, unlike $^3\Sigma$ states, the effective value of the angular momentum can deviate quite strongly from its initial value of unity and a proper description of the energy levels requires an explicit incorporation of the Coriolis terms and diagonalization of the appropriate matrix, a 2×2 matrix in the case of $j = 1$. The major effect of the Coriolis term is to remove the degeneracy of the $K = \pm 1$ and $K = \pm 2$ levels *etc.* for each j. Thus in the $j = 1$ state the $K = 0$ level is coupled to the symmetric combination of the eigenstates with $K = 1$ and $K = -1$. These symmetrized states are

$$| 1^+\rangle = \{| +1\rangle + | -1\rangle\}/\sqrt{2}, \tag{2}$$

$$| 1^-\rangle = \{| +1\rangle - | -1\rangle\}/\sqrt{2}. \tag{3}$$

The degeneracy of the $K = 1$ and $K = -1$ states is lifted by the Coriolis interaction, which only couples the $K = 0$ state to the symmetric combination $| 1^+\rangle$. The matrix element is

$$\langle 0 | \mathcal{H}_{\mathrm{Cor}} | 1^+\rangle = -\sqrt{2}B\sqrt{J(J+1)j^*(j^*+1)}, \tag{4}$$

where j^* is the effective value of j which is an empirical parameter determined from the fit. This pushes the $| 0\rangle$ and $| 1^+\rangle$ levels apart but leaves the $| 1^-\rangle$ unaffected. Taking the initial energies of the $K = 0$ and $K = \pm 1$ levels as $-\alpha$ and α, respectively, the energy levels are given by the eigenvalues of the 2×2 matrix

$$\mathcal{H} = \tag{5}$$

$$\begin{pmatrix} B_{K=0}J(J+1) - \alpha & -\sqrt{2}B\sqrt{j^*(j^*+1)J(J+1)} \\ -\sqrt{2}B\sqrt{j^*(j^*+1)J(J+1)} & B_{K=1}J(J+1) + \alpha \end{pmatrix},$$

where $B_{K=0}$ and $B_{K=1}$ are the rotational constants of the $K = 0$ and $K = \pm 1$ levels, respectively, and B is taken as the mean of these two values. Diagonalizing the 2×2 matrix gives the eigenvalues

$$E_J = E_\nu + \left(\frac{B_{K=0} + B_{K=1}}{2}\right) J(J+1) \tag{6}$$

$$\pm\frac{1}{2}\{4\alpha^2 + 4\alpha\Delta B J(J+1) + \Delta B^2 J^2(J+1)^2 + 8B^2 j^*(j^*+1)J(J+1)\}^{1/2},$$

where E_ν is the vibrational energy and $\Delta B = B_{K=1} - B_{K=0}$. There is often insufficient information to determine ΔB as it is highly correlated with the Coriolis term. In this case, constraining ΔB to zero, simplifies the above equation to

$$E_J = E_\nu + BJ(J+1) \pm \sqrt{\alpha^2 + 2B^2 j^*(j^*+1)J(J+1)}. \tag{7}$$

In the excited vibrational state, the rotational energy of the $| 1^-\rangle$ state is given by

$$E_J = E_\nu + \alpha + B_{K=1}J(J+1). \tag{8}$$

Starting in states correlating with $j = 0$, the selection rule on the total angular momentum is $\Delta J = \pm 1$ for transitions to the mixed $| 0\rangle$ and $| 1^+\rangle$ states and $\Delta J = 0$ to the $| 1^-\rangle$ states. The energies of the lower levels are $B'' J(J+1)$.

The rotational levels of CH_4 in the ground vibrational state and in the excited vibrational state ν_4 are represented in the left part of Figure 3. The rotational levels corresponding to the end over end rotation of the complex are built on top of the j, n levels of the CH_4 part (by definition $n = j$ in the ground state, and $n = j$, $j \pm 1$ in the ν_4 excited vibrational state), and are characterized by the J quantum number of the total angular momentum of the complex. The right part of Fig. 3 shows the splitting of one of the J levels in the upper vibrational state into three components $| 1^+\rangle$, $| 1^-\rangle$ and $| 0\rangle$.

The transitions shown in Figs. 1 and 2 for Ar–CH_4 and Kr–CH_4 were fitted to the above expressions for upper and lower states and making use of the fact that the strong $^Q\mathrm{R}_0$ and $^R\mathrm{P}_0$ branch lines terminate, respectively, in the lower $| 0\rangle$ and upper $| 1^+\rangle$ Coriolis coupled components, as it is shown in Figure 3. These transitions correlate with $\Delta N = 0$ selection rule in the limit of complete decoupling of j from

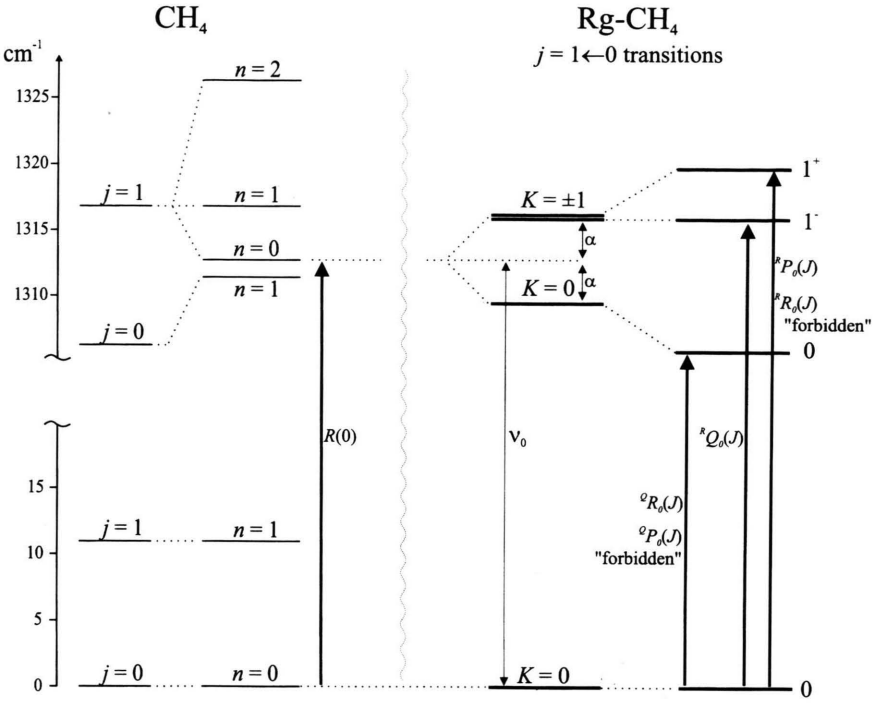

Fig. 3. Energy level diagram – to the left of the CH_4 monomer (in scale), to the right for the complex (not in scale; for details see text).

the intermolecular axis, where the quantum number N corresponds to the angular momentum of the end over end rotation of the complex. The lines were fitted to (6) and (8) using a Levenberg-Marquardt nonlinear least squares method [15]. A centrifugal quadratic distortion term, $-DJ^2(J+1)^2$, assumed to be the same in both vibrational states, was also taken into account, which enabled fitting the positions of the lines to the experimental accuracy.

However, because of strong correlation between rotational constants it was not possible to determine precisely the values of the rotational constants in the various states using only the transitions shown in Figs. 1 and 2. This can be understood in the following manner. As soon as the Coriolis term dominates over the initial splitting of the $K = 0$ and $K = \pm 1$ levels, their energies are given by

$$E_J = E_\nu + BJ(J+1) \pm \sqrt{2}B\sqrt{j^*(j^*+1)}(J+\frac{1}{2}). \quad (9)$$

So approximate expressions for the R and P branches are

$$\nu_R(J) = \nu_0 + B(J+1)(J+2) - \sqrt{2}B\sqrt{j^*(j^*+1)}(J+\frac{3}{2}) - B''J(J+1) \quad (10)$$

$$\nu_R(J) = \nu_0 - B\sqrt{\frac{1}{2}j^*(j^*+1)} + \left\{(B+B'') - B\sqrt{2j^*(j^*+1)}\right\}(J+1) + (B-B'')(J+1)^2$$

and

$$\nu_P(J) = \nu_0 + B(J-1)J + \sqrt{2}B\sqrt{j^*(j^*+1)}(J-\frac{1}{2}) - B''J(J+1) = \nu_0 - B\sqrt{\frac{1}{2}j^*(j^*+1)} - \left\{(B+B'') - B\sqrt{2j^*(j^*+1)}\right\}J + (B-B'')J^2. \quad (11)$$

As can be readily observed, both expressions depend on the same three combinations of constants, so that without further information it is not surprising that it is difficult to determine precise values of all variables. Two possibilities can be used to resolve this problem. One is to observe the microwave spectrum and determine the ground state rotational (and centrifugal distortion) constants directly. This would be the most

Table 1. Fitted parameters of Ar–CH_4 and Kr–CH_4 (cm^{-1}).

	$j = 1 \leftarrow 0$	
	Ar–CH_4	Kr–CH_4
ν_0	1310.798736 (77)	1310.458368 (70)
$B'_{K=1}$	0.092229 (11)	0.074813 (10)
$B'_{K=0}$	0.092331 (11)	0.074922 (11)
B''	0.092125 (11)	0.074713 (10)
α	0.19497 (13)	0.338232 (98)
$\sqrt{2}B'\sqrt{j^*(j^*+1)}$	0.170147 (48)	0.134747 (42)
D	$2.375(18)\cdot10^{-6}$	$1.6116(91)\cdot10^{-6}$
σ_{fit}	0.00022	0.00025

precise way which should be possible after having the rotational constants preliminarily determined, for example from the IR data. The direct search for the microwave transitions without such preliminary information is complicated by the weak intensity of the transitions due to the small permanent dipole moments of the complexes and also by the fact that it is not possible to identify the internal rotor state of methane (which is characterized by j) in which the microwave transitions occur.

An alternative approach is to observe the nearly forbidden $^QP_0$ or $^RR_0$ branches. The appropriate transitions are schematically shown in Fig. 3 together with the allowed $^RP_0$, $^RQ_0$ and $^QR_0$ transitions. Then by combination differences there is information on the ground state rotational constant.

The latter approach was used in the present work. After the strong allowed transitions were fitted, the positions of the low J "forbidden" transitions were predicted, which enabled observation of two $^QP_0$–branch lines and three $^RR_0$–branch lines in the case of Ar–CH_4, and five $^RR_0$-branch lines in the case of Kr–CH_4. The intensity of the observed nearly forbidden transitions relative to the strong allowed transitions is considerably lower than in the case of Ne–SiH_4 [10], which is partly due to the higher temperature of the jet in the Ar–CH_4 and Kr–CH_4 case (5–7 K in comparison with 0.5 K in the Ne–SiH_4 experiments), and also because of the lower anisotropy of the intermolecular potential in Ar–CH_4 and Kr–CH_4 compared to Ne–SiH_4. These transitions were then included in the final fit. The results of the fit are given in Table 1. The transitions for Ar–CH_4 and Kr–CH_4 are listed in Table 2 and Table 3, respectively. It should be noted that the use of the observed nearly forbidden transitions in the fit resulted in a relatively small change of the B constants (−0.3% and −0.2% for the ground state rotational constant B'' of Ar–CH_4 and Kr–CH_4, respectively).

4. Discussion

The spectra of Ar–CH_4 and Kr–CH_4 in the R(0) of the monomer have been analyzed in terms of a near free-rotor model. Accurate values of all B rotational constants in all states have been obtained. These constants can be used to determine the separation between methane and the rare gas atom; the values for the $j = 0$

Table 2. Observed line positions and the differences to the calculated positions of the $j = 1 \leftarrow 0$ band of Ar–CH_4 (values are in cm^{-1}).

	$^RP_0$		$^RQ_0$		$^QR_0$		$^QP_0$		$^RR_0$	
J	OBS	O–C	OBS	O–C	OBS	O–C	OBS	O–C	OBS	O–C
0					1310.6739	0.0003			1311.2931	0.0002
1					1310.7084	0.0004			1311.6283	0.0002
2	1310.7404	0.0001	1310.9946	0.0003	1310.7326	0.0002			1311.9744	0.0006
3	1310.7071	−0.0001	1310.9946	0.0003	1310.7531	0.0002				
4	1310.6849	−0.0000	1310.9958	0.0000	1310.7717	0.0002	1309.4438	0.0003		
5	1310.6671	−0.0000	1310.9969	0.0001	1310.7892	0.0001	1309.0968	0.0004		
6	1310.6516	−0.0003	1310.9982	0.0001	1310.8061	0.0001				
7	1310.6377	−0.0006	1310.9996	0.0001	1310.8221	−0.0003				
8	1310.6257	−0.0005	1311.0011	−0.0001	1310.8382	−0.0002				
9	1310.6147	−0.0005	1311.0031	0.0000	1310.8537	−0.0002				
10	1310.6048	−0.0005	1311.0051	−0.0000	1310.8687	−0.0004				
11	1310.5961	−0.0004	1311.0074	−0.0000	1310.8833	−0.0005				
12	1310.5886	−0.0002	1311.0099	−0.0000	1310.8974	−0.0006				
13	1310.5822	−0.0000	1311.0127	0.0001	1310.9114	−0.0004				
14	1310.5772	0.0004	1311.0156	0.0001	1310.9247	−0.0002				
15	1310.5733	0.0008	1311.0187	0.0000	1310.9375	−0.0000				
16			1311.0220	0.0000	1310.9499	0.0004				
17			1311.0255	−0.0000	1310.9615	0.0008				
18			1311.0293	0.0000						
19			1311.0331	−0.0001						

Table 3. Observed line positions and the differences to the calculated positions of the $j = 1 \leftarrow 0$ band of Kr–CH_4 (values are in cm^{-1}).

	$^RP_0$		$^RQ_0$		$^QR_0$		$^QP_0$	
J	OBS	O–C	OBS	O–C	OBS	O–C	OBS	O–C
0					1310.2196	−0.0003	1310.9964	0.0001
1					1310.2862	0.0006	1311.2307	0.0001
2	1310.5485	0.0005			1310.3328	0.0007	1311.4843	−0.0003
3	1310.4840	−0.0003	1310.7976	−0.0002	1310.3685	0.0005	1311.7498	0.0003
4	1310.4391	−0.0001	1310.7987	0.0001	1310.3984	0.0006	1312.0206	−0.0003
5	1310.4060	0.0001	1310.7999	0.0003	1310.4243	0.0003		
6	1310.3793	−0.0001	1310.8010	0.0002	1310.4478	0.0001		
7	1310.3570	−0.0002	1310.8024	0.0002	1310.4699	0.0001		
8	1310.3377	−0.0004	1310.8041	0.0002	1310.4909	−0.0002		
9	1310.3211	−0.0001	1310.8058	0.0001	1310.5107	−0.0002		
10	1310.3059	−0.0003	1310.8077	0.0000	1310.5298	−0.0003		
11	1310.2923	−0.0005	1310.8100	0.0001	1310.5485	−0.0002		
12	1310.2804	−0.0004	1310.8123	−0.0000	1310.5662	−0.0006		
13	1310.2694	−0.0007	1310.8150	0.0001	1310.5840	−0.0004		
14	1310.2602	−0.0003	1310.8178	0.0000	1310.6010	−0.0006		
15	1310.2520	−0.0001	1310.8207	−0.0001	1310.6176	−0.0006		
16	1310.2446	−0.0003	1310.8240	−0.0000	1310.6340	−0.0003		
17	1310.2390	0.0001	1310.8274	−0.0000	1310.6496	−0.0004		
18	1310.2344	0.0005	1310.8311	0.0000	1310.6649	−0.0002		
19	1310.2311	0.0009	1310.8349	0.0000	1310.6796	−0.0001		
20			1310.8389	−0.0000	1310.6942	0.0005		
21			1310.8429	−0.0003	1310.7083	0.0011		
22			1310.8476	0.0000				
23			1310.8521	−0.0001				
24			1310.8570	−0.0001				
25			1310.8622	0.0001				
26			1310.8675	0.0001				
27			1310.8728	0.0000				
28			1310.8785	−0.0003				

level of the ground vibrational state are 3.999 Å and 4.094 Å for Ar–CH_4 and Kr–CH_4, respectively. The difference between these two values largely reflects the difference in the size of the rare gas atom.

If compared to the Ne–SiH_4 complex, both Ar–CH_4 and Kr–CH_4 display quite small differences in the rotational constants between the $K = 0$ and $K = \pm 1$ states. This may reflect smaller consequences of the effects of the anisotropy of the intermolecular potential. Such smaller anisotropy effects also manifest themselves in the value of j^*. For the methane complexes it is much closer to the free rotation value of 1 (0.90 for Ar–CH_4 and 0.87 for Kr–CH_4) than in the Ne–SiH_4 ($j^* = 0.53$). This deviation from $j^* = 1$ is a consequence of the mixing of states of higher j into the monomer rotational functions for $K = 0$ and $K = \pm 1$. This depends upon both the anisotropy of the potential and the separation of the monomer levels involved. In first order perturbation theory we obtain approximate corrections, and in second order corrections to the energy levels that yield the splittings observed. It is clear that the larger values of the methane rotational constant (5.25 cm^{-1} as compared to 2.96 cm^{-1} for SiH_4) is important. However the much larger Coriolis splittings in the $v_4 = 1$ level of CH_4 also contribute (see Figure 3). A precise evaluation of these effects requires a detailed analysis of the hindered rotor dynamics.

Another important difference between Rg–CH_4 and Ne–SiH_4 is the totally different appearance of the bands. The lower prominence of the "forbidden" $^RR_0$ and $^QP_0$ branches in Ar–CH_4 and Kr–CH_4 would appear to be a consequence of the near free-rotor behaviour of the methane. The strong Coriolis mixing of the states with $K = 0$ and $K = \pm 1$ leads to the restriction of K as a good quantum number and leads to a new quantum number N where $\boldsymbol{N} = \boldsymbol{J} - \boldsymbol{j}$. The selection rule $\Delta N = 0$ leads to the apparent "Q-branch" appearance of the bands in the spectrum.

However all of this depends upon the relative magnitude of the Coriolis mixing term $\sqrt{2}Bj^*(j^* + 1) \cdot J(J + 1)$ and the splitting 2α. A measure of the importance of this effect for a given J is given by the value of $\sqrt{2}Bj^*(j^* + 1)/2\alpha$. The values are 0.436, 0.199 and 0.156 for Ar–CH_4, Kr–CH_4 and Ne–SiH_4, respectively, while it is clear that Coriolis effects are

most important in Ar–CH_4; the results for Kr–CH_4 and Ne–SiH_4 are very similar. The decay of the intrinsic intensity of the $^RR_0$ and $^QP_0$ branches should decay in a similar way for the last two molecules. The essential difference in the appearance of their spectra results from the great difference in the temperatures of the two species. The rotational temperature of Ne–SiH_4 in the spectra of [11] is close to 0.5 K, so that only the lowest rotational levels are observed. For the lowest rotational levels the effects of Coriolis mixing are smallest and the asymmetry between the "allowed"/"forbidden" P and R branches is minimal: For the Ar–CH_4 and Kr–CH_4 case observed presently, the beam temperature is in the range 5-7 K and the rotational population maximizes in the region of $J = 5 - 6$. For such levels Coriolis effects are dominant and the intensity of $^RR_0$ or $^QP_0$ is very small compared to the corresponding $^RP_0$ or $^QR_0$ and the asymmetry is most pronounced.

We also have performed measurements on the $j = 0 \leftarrow 1$ transitions of Ar–CH_4 and Kr–CH_4 correlated with the P(1), Q(1) and R(1) transitions of methane. The analysis of the data is in progress and will be presented in a separate paper. The combined results should help to enable the determination of the potential parameters which characterize the anisotropic part of the intermolecular potential.

Acknowledgements

We would like to thank M. Wangler for his help in the experiments. The work of I. P. at Cologne was made possible by the Deutsche Forschungsgemeinschaft through a grant aimed to support Eastern and Central European Countries and the Republics of the former Soviet Union. The work was supported by the Deutsche Forschungsgemeinschaft via Research Grant SFB–301. D. S. thanks the EPSRC (UK) for a studentship.

[1] A. R. W. McKellar, Faraday Discuss. Chem. Soc. **97,** 69 (1994).
[2] C. M. Lovejoy and D. J. Nesbitt, Faraday Discuss. Chem. Soc. **97,** 175 (1994).
[3] P. A. Block and R. E. Miller, Faraday Discuss. Chem. Soc. **97,** 177 (1994).
[4] B. J. Howard (personal communication, 1996)
[5] I. Pak, M. Hepp, D. A. Roth, G. Winnewisser, and K. M. T. Yamada, Z. Naturforsch. **51a,** 997 (1996).
[6] I. Pak, M. Hepp, D. A. Roth, and G. Winnewisser, Rev. Sci. Instrum. **68,** 1668 (1997).
[7] R.-D. Urban, L. G. Jörissen, Y. Matsumoto, and M. Takami, J. Chem. Phys. **103,** 3960 (1995).
[8] E. J. Bieske, S. A. Nizkorodov, O. Dopfer, J. P. Maier, R. J. Stickland, B. J. Cotterell, and B. J. Howard, Chem. Phys. Letters **250**, 266 (1996).
[9] O. Dopfer, S. A. Nizkorodov, M. Meuwly, E. J. Bieske, and J. P. Maier, Chem. Phys. Letters **260**, 545 (1996).
[10] R. W. Randall, J. B. Ibbotson, and B. J. Howard, J. Chem. Phys. **100,** 7051 (1994).
[11] M. D. Brookes, D. J. Hughes and B. J. Howard, J. Chem. Phys. **104,** 5391 (1996).
[12] M. D. Brookes, D. J. Hughes and B. J. Howard, J. Chem. Phys. **107,** 2738 (1997).
[13] R. W. Randall, J. B. Ibbotson, and B. J. Howard, J. Chem. Phys. **100,** 7042 (1994).
[14] I. Pak, M. Hepp, R. Philipp, R. Schieder, and G. Winnewisser, Z. Naturforsch. **49a,** 913 (1994).
[15] W. H. Press, S. A. Teukolsky, W. T. Vetterling, and B. P. Flannery, Numerical Recipes in C, Cambridge University, Cambridge 1992, p. 683.

Verantwortlich für den Inhalt: A. KLEMM
Satz und Druck: Konrad Triltsch, Würzburg